IOPscience iopscience.iop.org

Home Search Collections Journals About Contact us My IOPscience

Passivation of hexagonal SiC surfaces by hydrogen termination

This article has been downloaded from IOPscience. Please scroll down to see the full text article.

2004 J. Phys.: Condens. Matter 16 S1755

(http://iopscience.iop.org/0953-8984/16/17/016)

View the table of contents for this issue, or go to the journal homepage for more

Download details:
IP Address: 129.252.86.83
The article was downloaded on 27/05/2010 at 14:31

Please note that terms and conditions apply.

INSTITUTE OF PHYSICS PUBLISHING JOURNAL OF PHYSICS: CONDENSED MATTER

J. Phys.: Condens. Matter **16** (2004) S1755–S1782 PII: S0953-8984(04)65147-2

Passivation of hexagonal SiC surfaces by hydrogen termination

Thomas Seyller

Universität Erlangen-Nürnberg, Institut für Technische Physik,
Lehrstuhl für Experimentalphysik, Erwin-Rommel-Straße 1, 91058 Erlangen, Germany

E-mail: thomas.seyller@physik.uni.erlangen.de

Received 24 June 2003
Published 16 April 2004
Online at stacks.iop.org/JPhysCM/16/S1755
DOI: 10.1088/0953-8984/16/17/016

Abstract

Surface hydrogenation is a well established technique in silicon technology. It is easily accomplished by wet-chemical procedures and results in clean and unreconstructed surfaces, which are extremely low in charged surface states and stable against oxidation in air, thus constituting an ideal surface preparation. As a consequence, methods for hydrogenation have been sought for preparing silicon carbide (SiC) surfaces with similar well defined properties. It was soon recognized, however, that due to different surface chemistry new ground had to be broken in order to find a method leading to the desired monatomic hydrogen saturation. In this paper the results of H passivation of SiC surfaces by high-temperature hydrogen annealing will be discussed, thereby placing emphasis on chemical, structural and electronic properties of the resulting surfaces. In addition to their unique properties, hydrogenated hexagonal SiC{0001} surfaces offer the interesting possibility of gaining insight into the formation of silicon- and carbon-rich reconstructions as well. This is due to the fact that to date hydrogenation is the only method providing oxygen-free surfaces with a C to Si ratio of 1:1. Last but not least, the electronic properties of hydrogen-free SiC{0001} surfaces will be alluded to. SiC{0001} surfaces are the only known semiconductor surfaces that can be prepared in their unreconstructed (1×1) state with one dangling bond per unit cell by photon induced hydrogen desorption. These surfaces give indications of a Mott–Hubbard surface band structure.

1. Introduction

On account of its physical properties, the wide-bandgap semiconductor silicon carbide (SiC) is a promising material for electronic devices suitable for high-power, high-temperature and high-frequency applications. The new generation of electronic devices which is about to

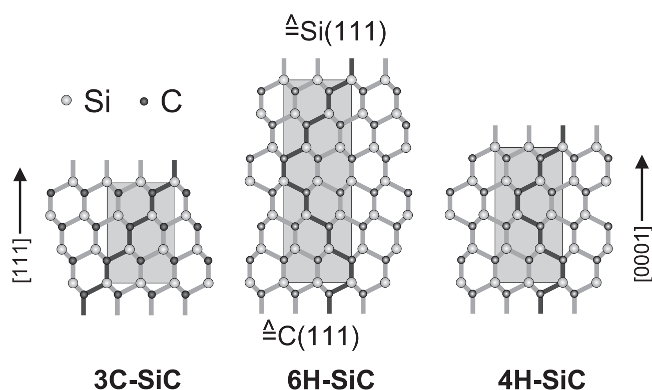

Figure 1. Crystal structure of the three most commonly studied polytypes 3C-, 4H-, and 6H-SiC in a side view projection. The 3C-SiC(111) and the 4H- and 6H-SiC(0001) surfaces are structurally equivalent to the Si(111) surface in that they consist of Si atoms only (silicon face). The carbon face which faces the opposite direction is equivalent to the diamond C(111) surface.

emerge will exhibit higher compactness, improved reliability, higher voltage ratings and higher efficiency than conventional Si based devices. Possible applications of such electronic devices would be beneficial for communication electronics, multimedia devices, server applications, transportation, engine sensors in cars or aircraft and many more. In some of these areas SiC devices are already in use.

For future development of such devices, a surface preparation technique is required which yields clean and well ordered surfaces and which provides good chemical stability between processing steps. In Si technology these requirements are fulfilled by surface hydrogenation, a well established technique which is accomplished by wet-chemical methods [1] involving hydrofluoric acid (HF) or buffered HF solutions. The resulting hydrogen layer serves as a means to prevent contamination of the surfaces between processing steps [1]. On Si(111) it was observed that etching the surface in buffered NH_4F solution (BHF) leads to extremely flat surfaces, which are unreconstructed and ideally H terminated by Si–H entities only [2]. In addition, the H terminated Si surfaces exhibit extremely few charged surface states [3], leading to an unpinned surface Fermi level [4]. Yablonovitch *et al* [3] reported a record low of 2.5×10^7 charged surface states cm^{-2} for hydrogenated Si(111). The hydrogen terminated Si surfaces are also well protected against oxidation in air [3, 5].

Considering the crystal structure of SiC (see figure 1), it is evident that the (0001) surfaces of the hexagonal polytypes 4H- and 6H-SiC, which are mainly used for applications so far, are structurally equivalent to the Si(111) surface. Therefore, and in view of the promising results on Si(111), it is no surprise that surface hydrogenation has also been tried on hexagonal SiC{0001} surfaces using initially the same methods which work so well on Si(111).

However, the wet-chemical recipes do not yield the desired monohydride coverage on SiC{0001} surfaces. According to a number of studies [6–18], HF or BHF treated surfaces exhibiting a (1×1) diffraction pattern in low-energy electron diffraction (LEED) contain a considerable amount of oxygen as determined by Auger electron spectroscopy (AES), x-ray induced photoelectron spectroscopy (XPS) or soft x-ray photoelectron spectroscopy (SXPS). In some cases the presence of fluorine was also reported. The XPS and SXPS data [10, 17, 18] indicated that in all cases an oxygen coverage of the order of one monolayer was present. In addition, the surfaces contained varying amounts of excess carbon [9, 10, 17, 18] in the form of hydrocarbons. Surface Si–H bonds were not observed by high-resolution electron energy

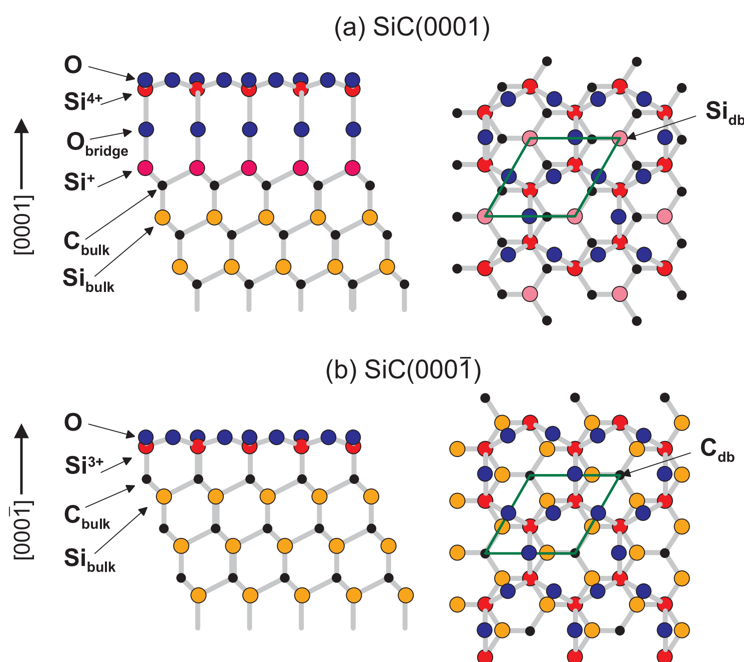

Figure 2. Structural models of the silicate adlayer reconstructions on SiC(0001) and (000$\bar{1}$) as determined by LEED [22, 23]. Drawing not to scale.

(This figure is in colour only in the electronic version)

loss spectroscopy (HREELS) [9] or by Fourier-transform infrared absorption spectroscopy (FTIR) [13–16]. On the other hand, these vibrational spectroscopic techniques provided evidence for the presence of hydroxyl groups on the HF and BHF treated surfaces [9, 16]. In a dynamical LEED study carried out by the group of Starke *et al* [8], the HF treated 6H-SiC(0001) surface was found to be terminated by a monolayer of oxygen atoms located in on-top positions above the Si atoms of the topmost bilayer. This bonding configuration would indeed be expected for a bulk terminated SiC(0001) surface with the dangling bonds of the top Si atoms saturated by OH groups. The picture which emerges from the results summarized above is that the HF and BHF treated SiC(0001) surfaces are essentially OH terminated. Similar observations were made on the SiC(000$\bar{1}$) surface, the so-called carbon face. In this case oxygen is present on the surface as well, indicating that wet-chemical treatment is also not successful on this surface [6, 12, 17–19]. The oxygen contamination on both SiC(0001) and SiC(000$\bar{1}$) can only be removed if the sample is heated to temperatures of about 900–1000 °C, which also leads to the formation of reconstructed surfaces (see section 6), making this surface preparation inadequate for a technical process.

A further attempt to hydrogenate SiC surfaces was made by using a hydrogen plasma. This method works well on diamond surfaces [20, 21] but in the case of SiC{0001} the resulting surfaces are covered by a monolayer of well ordered silicon oxide [17, 22–25] presumably due to a residual oxygen contamination of the process gas (see also section 2). The structure of these ordered oxides on SiC{0001} surfaces was determined by LEED [22, 23] and is shown in figure 2. According to the LEED study, this so-called silicate adlayer consists of a surface layer in which the Si atoms (labelled Si^{4+} in figure 2(a) and Si^{3+} in figure 2(b)) are bound to three oxygen atoms within the same layer (labelled O) thus forming hexagonal rings. This

layer is connected to the Si face by bridging oxygen atoms (O_{bridge}). On the C face the silicate layer is bound directly to the topmost carbon layer. The Si/C atoms of the top Si/C layer of SiC(0001) and (000$\bar{1}$), respectively, which are located in the centre of the rings, exhibit a dangling bond (db). These are labelled Si_{db} and C_{db}, respectively. The silicate adlayer structures were studied by Hollering *et al* [24, 25] and Sieber *et al* [17, 26] using SXPS and UPS. An analysis of the chemically shifted components in the Si 2p and C 1s core level spectra confirmed the structural models proposed in the LEED study [22, 23]. In addition, Hollering *et al* [24, 25] observed the db state on the silicate adlayer reconstructed 6H-SiC(000$\bar{1}$) surface. It is located energetically above the valence band maximum (VBM) but below the Fermi level. This behaviour can be explained by a Mott–Hubbard metal–insulator transition. A later DFT study [27, 28] confirmed these experimental observations. It also found that on the C face a structure without bridging oxygen atoms is energetically favourable compared to the structure with the bridging oxygen atoms, which is in contrast to the situation on the Si face.

Van Elsbergen *et al* [29] tried to prepare hydrogen saturated SiC(0001) surfaces by exposing the ($\sqrt{3} \times \sqrt{3}$) reconstructed surface to atomic hydrogen which was generated by cracking molecular hydrogen on a hot tungsten filament in ultra-high vacuum (UHV). After this the reconstruction was lifted and the surfaces exhibited a (1×1) periodicity in LEED. The oxygen uptake was measured by taking XPS spectra after exposing the samples to molecular oxygen at room temperature. In this way a drastically reduced oxygen uptake as compared to the ($\sqrt{3} \times \sqrt{3}$) reconstructed surface was observed which led the authors to the conclusion that the surface was successfully hydrogenated, albeit no direct spectroscopic evidence was given for the presence of hydrogen on the surface. Later it was shown by HREELS [30, 31] that the method used by van Elsbergen and co-workers [29] indeed produces surface Si–H bonds when applied to Si-rich (3×3) and ($\sqrt{3} \times \sqrt{3}$) surfaces. However, it is unclear to what extent the surface bonds were saturated by hydrogen, i.e. whether the surface was completely saturated with hydrogen or whether it was only partially hydrogenated. Besides, the method for hydrogenation employed by van Elsbergen *et al* [29], Tautz *et al* [30] and Stoldt *et al* [31] does not seem suitable for technological processes for obvious reasons.

Another method for hydrogenation, which has been proven to yield SiC{0001} surfaces saturated with a monolayer of hydrogen, was first suggested by Tsuchida *et al* [13–16], who annealed SiC{0001} samples in an atmosphere of ultra-clean hydrogen at temperatures of 1000 °C and above. This procedure is similar to the hydrogen etching which is widely used to reduce surface roughness and polishing damage of SiC substrate surfaces prior to homoepitaxial growth by chemical vapour deposition (CVD) [32, 33]; it was subsequently used in our group to prepare hydrogenated SiC surfaces. The advantage of the method used by Tsuchida *et al* [13–16] and by our group is that it can be carried out in a SiC CVD reactor provided that the hydrogen used for the procedure is extremely clean (grade 8.0).

The present paper summarizes the current knowledge about the properties of H terminated, hexagonal SiC surfaces which were prepared by high-temperature hydrogen annealing. In section 2 experimental considerations will be discussed briefly. Section 3 will show that the technique described in section 2 results in clean, well ordered and hydrogen terminated SiC surfaces. In section 4 the chemical passivation of hexagonal SiC surfaces by hydrogen will be discussed. As will be shown in section 5, the analysis of Si–H stretch modes on 6H-SiC(0001) and 3C-SiC(111) leads to interesting results concerning the stacking sequence of the SiC crystal below the surface. In section 6 the thermal desorption of hydrogen will be discussed. The outstanding aspect of the hydrogen passivated SiC{0001} surfaces is that they provide a stoichiometric and oxygen-free starting point for the thermally induced formation of reconstructed surfaces, i.e. the ($\sqrt{3} \times \sqrt{3}$)R30° and (3×3) reconstructions on 6H-SiC(0001) and 6H-SiC(000$\bar{1}$), respectively. This provides new insights into how these reconstructions

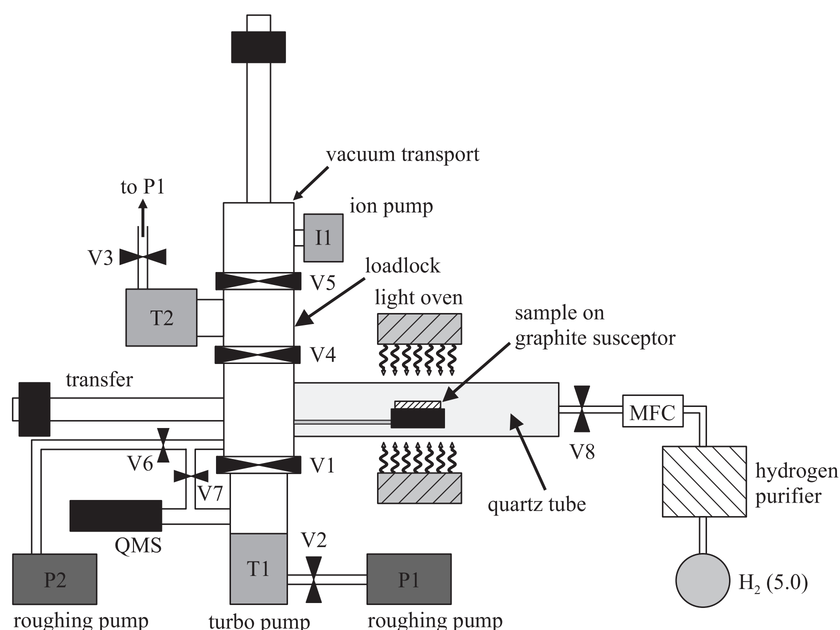

Figure 3. Sketch of the custom designed apparatus used in our group for hydrogenation of SiC surfaces [34].

are formed and into the origin of the surface components observed in the Si 2p and C 1s core level spectra of these reconstructions. In addition to thermally induced hydrogen desorption, section 7 will briefly discuss how photon induced hydrogen desorption can be used to prepare unreconstructed SiC{0001}-(1×1) surfaces with one db per unit cell. The topic of section 8 will be the electronic passivation of SiC{0001} surfaces by hydrogenation. Finally, section 9 gives a brief summary and an outlook on interesting questions for future investigations.

2. Experimental considerations

As mentioned in section 1, hydrogenation of SiC surfaces can be accomplished by annealing the samples in ultra-pure hydrogen at temperatures around 1000 °C. Tsuchida and co-workers [13–16] were the first to demonstrate successfully the presence of Si–H and C–H bonds on 6H-SiC(0001) and (000$\bar{1}$) prepared by high-temperature hydrogen annealing, respectively. For this purpose they used a SiC CVD reactor with a base pressure of 6×10^{-8} mbar. Hydrogen was purified by a palladium diffusion cell. The on-axis cut, polished 6H-SiC{0001} samples from CREE Inc. were annealed by high-frequency inductive heating at temperatures between 800 and 1200 °C for 30 min in 1 bar of hydrogen under a flow of 5 standard litres per minute (slm). Heating and cooling rates were 30 °C min^{-1}. The samples were analysed for Si–H and C–H bonds using Fourier-transform infrared absorption spectroscopy in the attenuated total reflection mode (FTIR-ATR) and atomic force microscopy (AFM). No other surface sensitive analysis techniques were used.

The same principle of operation was used in our group in order to hydrogenate SiC surfaces, but using a custom designed system [34] which is shown in figure 3. The reactor itself consists of a quartz tube. A graphite susceptor in the centre of the tube carries the Mo sample holder on which the SiC samples of about 5 mm $\times$ 8 mm size are clamped and which is compatible with the sample holder systems in the different analysis chambers in our laboratory. Heating to temperatures of up to 1200 °C is accomplished by a light oven with five halogen lamps

and a total heating power of 5 kW. The apparatus with a base pressure below 1×10^{-8} mbar is equipped with a load lock for fast sample entry and a quadrupole mass spectrometer for monitoring residual as well as process gas composition. Hydrogen of grade 5.0 is purified to grade 8.0 by means of a Pd diffusion cell. Note that using hydrogen of lower purity leads to the formation of the silicate adlayer reconstruction [22, 23, 26]. A transportable UHV chamber ($p < 1 \times 10^{-8}$ mbar) with a mobile ion pump can be attached to the apparatus. Using this UHV transport system, SiC samples can be transported to the different experimental stations in our home laboratory and to the synchrotron radiation source BESSY II without exposure to air.

Our studies of hydrogenated SiC surfaces concentrated on the basal planes of 6H-SiC, i.e. the C terminated SiC$(000\bar{1})$ surface and the Si terminated SiC(0001) surface. Si terminated samples from CREE Research, Inc. were used which were either polished substrates (n-type) or homoeptaxial epilayers (n- and p-type). Both types were oriented 3.5° off-axis. The effective doping concentrations were $N_D^{eff} = 1.4 \times 10^{18}$ cm^{-3} (n-type substrate) as well as $N_D^{eff} = 2 \times 10^{16}$ cm^{-3} (n-type epi) and $N_A^{eff} = 1 \times 10^{16}$ cm^{-3} (p-type epi), respectively. The C terminated samples were all n-type and on-axis oriented. Crystals were obtained from SiCrystal (polished substrates, $N_D^{eff} = 5 \times 10^{18}$ cm^{-3}) and CREE Research, Inc. (epilayers, $N_D^{eff} = 5 \times 10^{18}$ cm^{-3}). In addition, we also used heteroepitaxial 3C-SiC films of various orientations ((111), (100), (110)) on Si substrates provided by Dr C A Zorman from the Department of Electrical Engineering and Computer Science, Case Western Reserve University. With the help of these samples the etch rate of SiC was determined for the conditions used in our hydrogenation process.

Before hydrogenation, the samples were cleaned by a four-step wet-chemical treatment [18]. It consists of step A, 10 min in a 4:1 mixture of H_2SO_4 (97%) and H_2O_2 (30%) (Piranha solution) at 180 °C; step B, 10 min in HF (40%) at room temperature; step C, 10 min in a 4:1:1 mixture of H_2O, H_2O_2 (30%) and HCl (37%) at 80 °C; step D, 5 min in HF (5%) at room temperature. Each step is followed by rinsing in deionized water. Step A of the wet-chemical procedure removes contamination by organics and step C is intended to dissolve metals from the surface [1]. Steps B and D are supposed to etch silicon dioxide.

The hydrogenation process was carried out by first ramping the temperature to the desired value within 3 min, keeping the hydrogen pressure at around 0.1 bar and the flow rate at 1.5 slm. After increasing the pressure to 1 bar the flow was reduced to zero and the samples were annealed for 15 min under these conditions. The samples were then allowed to cool to room temperature in the hydrogen ambient using different cooling rates. Then hydrogen was pumped off and the samples were analysed. Note, that the hydrogen flux during the annealing cycle does not influence the surface properties, i.e. zero flux leads to the same results as keeping the flux at 1.5 slm during the entire procedure. For the determination of the SiC etch rate extended annealing times were used.

In order to gain information about the hydrogenated SiC surfaces we applied FTIR-ATR, XPS, SXPS, UPS, LEED and AFM. FTIR-ATR spectra of the Si–H and C–H stretch modes were collected with a Perkin Elmer Spectrum 2000 FTIR spectrometer. The measurements were carried out *ex situ* using a germanium prism as a multiple internal reflection element. XPS measurements in our home laboratory were obtained using monochromatized Al Kα radiation and an SSI electron analyser yielding an overall resolution of 0.6 eV. SXPS data were collected at BESSY II (beam line U49/2-PGM2 as well as UE56/2-PGM1 and 2) using two different end stations provided by the group of Professor Dr Schmeisser, BTU Cottbus and by Dr Martin Polcik from the Fritz–Haber-Institute. Determination of the thickness of epitaxial 3C-SiC films on Si substrates after hydrogen treatment was accomplished by spectroscopic ellipsometry using a J A Woolam M-44 ellipsometer.

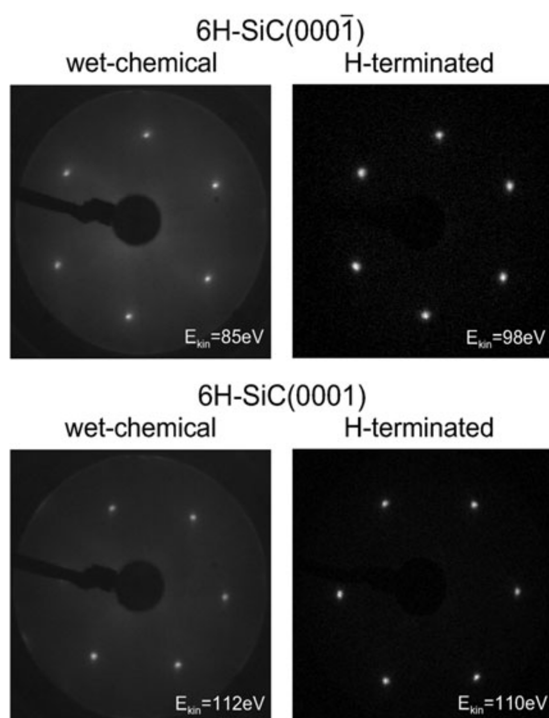

Figure 4. LEED patterns of 6H-SiC(000$\bar{1}$) (top) and 6H-SiC(0001) (bottom) after wet-chemical cleaning (left) and hydrogenation by annealing in ultra-pure hydrogen (right).

3. Composition and structure of hydrogenated 6H-SiC{0001} surfaces

In this section the chemical composition and the structural properties of the hydrogenated SiC{0001} surfaces will be discussed. Whereas contaminants like oxygen and fluorine can easily be detected by electron spectroscopy (AES, XPS, SXPS) these methods cannot unambiguously prove the presence of hydrogen. On the other hand, this is readily accomplished by infrared absorption spectroscopy (IRAS). In addition to the verification of successful hydrogenation, IRAS provides a wealth of information about structural and chemical properties of surfaces, as discussed in a recent review by Chabal and Raghavachari [35] for the case of hydrogenated silicon surfaces. Consequently, XPS/SXPS and FTIR-ATR are complementary methods, which in combination provide the maximum amount of information. In addition, LEED provides information about surface periodicity and thus has been used together with the other techniques to develop structural models for the surfaces under consideration.

3.1. Structural characterization by low-energy electron diffraction

Representative LEED patterns of 6H-SiC(0001) and (000$\bar{1}$) surfaces after wet-chemical pre-cleaning (see section 2) and hydrogenation are shown in figure 4. All four diffraction patterns show a (1×1) periodicity with quite sharp diffraction spots. In all our experiments it was observed that the diffraction patterns of the wet-chemically cleaned surfaces displayed a higher diffuse-elastic background than the diffraction patterns of the hydrogenated surfaces. This may be due to the contaminations (oxygen, fluorine and hydrocarbons) present after the HF dip. As a matter of fact, the LEED patterns of the hydrogenated surfaces were observed to possess an extremely low background, indicating a high degree of order on the surfaces.

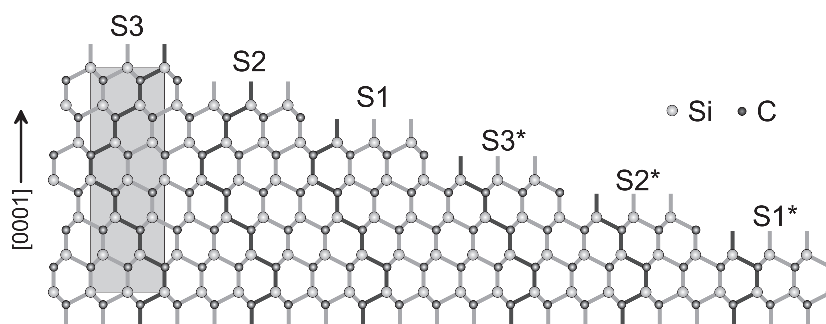

Figure 5. The three inequivalent terminations S1, S2 and S3 of 6H-SiC(0001) together with the equivalent S1*, S2* and S3* terminations shown in a side view projection.

In addition, the LEED patterns exhibit a sixfold rotational symmetry, in agreement with previous LEED studies of 6H-SiC{0001} surfaces [8, 9]. Considering the crystal structure of 6H-SiC (see figure 5), there are three possible inequivalent surfaces, which are denoted S1, S2 and S3 [8]. The number indicates the position of the next hexagonal stacking with respect to the surface, i.e. the number of bilayers between the surface and the next hexagonal stacking sequence. In addition, there are three further surfaces S1*, S2* and S3*, which in terms of stacking sequence are equivalent to S1, S2 and S3, respectively, but which can be obtained from the latter by a rotation by 60° around the surface normal. The diffraction pattern of a single domain (0001) or (000$\bar{1}$) surface, e.g. a surface with sole S1 termination, would be expected to have threefold rotational symmetry. However, the presence of domains with equivalent termination in equal fractions, e.g. S1 and S1*, leads to a diffraction pattern with sixfold rotational symmetry. Such a surface would exhibit step heights equivalent to three bilayers (or integer multiples thereof), whereas a single domain surface would possess step heights equal to integer multiples of six bilayers. The observation of step height of integer multiples of three bilayers on wet-chemically prepared 6H-SiC(0001) indicates that there is no preference for either of the two possible, equivalent terminations [8, 9]. However, a preference for S3/S3* termination was found as discussed elsewhere [8, 9]. The observation of sixfold rotational symmetry in the LEED patterns of our wet-chemically treated and H terminated samples thus shows that in our case, too, there is no preference for either of the two equivalent surface terminations. That there may indeed be a preference for a certain stacking (S1/S1*, S2/S2* or S3/S3*) at the H terminated surfaces can be derived from the FTIR-ATR spectra, as will be discussed in section 5.

A somewhat different observation was reported by Owman *et al* [33]. They have used hydrogen etching at 1550° in order to remove polishing damage from 6H-SiC(0001) substrates [32, 33]. After transfer of the samples into a UHV analysis chamber, they observed a (1 × 1) LEED pattern with threefold rotational symmetry indicative of a single domain surface. In agreement with that, STM measurements show a preference for 6 bilayer high steps. No evidence was given for the presence of Si–H bonds on the surface and the purity of the hydrogen used was not stated. Therefore one can only speculate whether or not the surfaces were H terminated. The observation of a threefold LEED pattern, however, seems to indicate that hydrogen etching at higher temperatures than the ones used in our studies induces a preference for single-domain surfaces.

3.2. *Identification of dangling bond saturation with hydrogen by FTIR-ATR*

According to the crystal structure of SiC (see figure 1) the hydrogenation of 6H-SiC(0001) and (000$\bar{1}$) surfaces should lead to saturation of the Si and C dangling bonds by hydrogen,

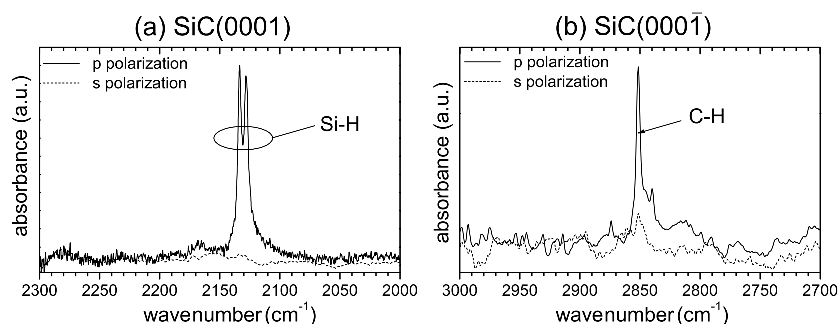

Figure 6. FTIR-ATR spectra of the Si–H and C–H stretch mode of hydrogenated 6H-SiC(0001) and $(000\bar{1})$, respectively.

respectively, which should be easy to identify by the corresponding absorption bands due to the Si–H or C–H stretch mode in infrared absorption. However, the extremely low concentration of hydrogen bonds compared to bulk samples requires measurements in the attenuated total reflection (FTIR-ATR) mode, in order to provide the necessary surface sensitivity.

Such measurements of hydrogenated 6H-SiC{0001} surfaces were first carried out by Tsuchida *et al* [13–16]. After their wet-chemical cleaning procedure (BHF dip) no Si–H bonds could be observed on both Si and C face. However, broad signals due to various CH_2 and CH_3 stretch modes of adsorbed hydrocarbons were always observed on both surface orientations. As will be discussed in section 4, these are due to adsorption of hydrocarbons from the atmosphere. First signs of hydrogen present on the SiC(0001) surfaces were seen after annealing in H_2 at 800 °C. The observed frequencies indicated Si–H bonds in the form of C_3SiH, C_2SiH_2 and $CSiH_3$ configurations, which would be expected for a microscopically rough surface. In addition, configurations with oxygen in backbonds, i.e. O_3SiH, O_2CSiH_2 and OC_2SiH_3, were also detectable. This indicates the presence of residual intermediate oxides and an incomplete hydrogenation. The latter absorption signals vanished after hydrogenation at 900 °C. At a preparation temperature of 1000 °C the SiC(0001) surface showed a sharp Si–H stretch mode at 2129 cm^{-1}, which broadened upon further increase of the preparation temperature. On the carbon face a sharp C–H stretch mode was observed at 2850 cm^{-1} after annealing in hydrogen at 1000–1200 °C. All these observations could be confirmed in our studies [34, 36].

Figure 6(a) displays the FTIR-ATR spectrum of the Si–H stretch mode on 6H-SiC(0001) after hydrogenation at 1000 °C. As can be seen from that figure, the absorption band due to Si–H monohydrides, which is only visible in p-polarization, consists of two narrow (FWHM of 3.0 cm^{-1}) lines at 2128.0 ± 0.6 and 2133.5 ± 0.6 cm^{-1}. The origin of this splitting will be discussed in section 5. At best, traces of Si–H_2 and Si–H_3 can be detected. Configurations with oxygen in the backbond are below the detection limit in agreement with the XPS and SXPS data (see section 3.3). This points towards an ideal monohydride termination of the surface. On the carbon face the hydrogenation leads to the appearance of a sharp absorption line at 2851.0 cm^{-1} (see figure 6(b)) due to C–H monohydrides, again in agreement with Tsuchida *et al* [13–16]. The small width of the signal (FWHM of 3.0 cm^{-1}) points towards a high degree of order on the surface. As observed with the Si–H stretch mode on 6H-SiC(0001) the absorption line due to the C–H stretch mode on $SiC(000\bar{1})$ appears only when the measurement is performed in p-polarization. This indicates that the respective Si–H and C–H bonds are perpendicular to the surface.

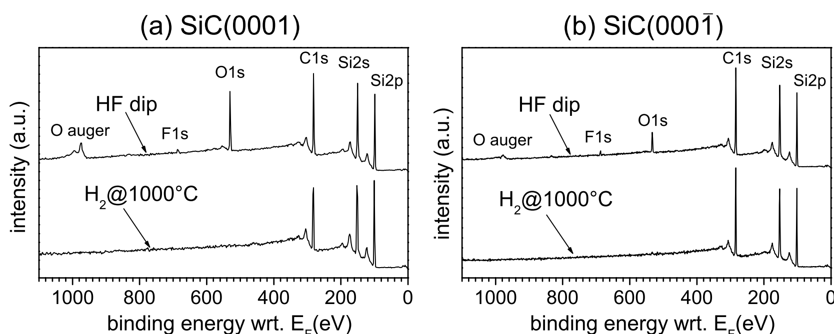

Figure 7. XPS survey scans of (a) p-type SiC(0001) and (b) n-type SiC(000$\bar{1}$) after wet-chemical cleaning (HF dip, upper spectra) and after hydrogenation at 1000 °C (lower spectra).

3.3. Characterization by photoelectron spectroscopy

3.3.1. Chemical composition determined by XPS. As discussed earlier, the wet-chemical pre-cleaning of the samples leads to the presence of oxygen and fluorine contamination on the surface. This is demonstrated in figures 7(a) and (b), where XPS survey scans are shown, which were taken from 6H-SiC(0001) and (000$\bar{1}$) samples, respectively. Spectra obtained before and after thermal hydrogenation at 1000 °C are displayed. The spectra of the wet-chemically prepared samples show clear signals due to fluorine and oxygen. In addition, a quantitative evaluation of these spectra indicates that the carbon content of the surfaces is higher than expected for stoichiometric SiC, due to adsorbed hydrocarbons (see below).

Annealing in hydrogen at temperatures above 950 °C leads to the effective removal of these contaminations [17, 34, 37–39]. This is clearly seen from the spectra taken after hydrogenation at 1000 °C. On both SiC(0001) and (000$\bar{1}$) signals due to oxygen are pushed below the detection limit which is 0.2 at.%. Note that on the silicon face the Si 2p line appears to be larger than the C 1s signal. On the carbon face a reverse behaviour is observed, i.e. the C 1s signal seems more intense than the Si 2p core level. This behaviour can be explained by considering that in the case of SiC(0001) the Si atoms in every single bilayer are located physically above the C atoms of the same bilayer (see figure 1). Therefore the photoelectrons from the carbon atoms suffer an additional damping by the Si atoms in the same bilayer, leading to a smaller relative C 1s signal. On the carbon face the role of Si and C atoms is reversed and so are the core line intensities. A proper quantitative analysis requires a correction for the spectrometer transmission function and the photoionization cross sections. Considering the spectrometer transmission function we obtain corrected Si 2p/C 1s intensity ratios of 1.09 and 0.93 for H terminated SiC(0001) and SiC(000$\bar{1}$), respectively. On the other hand, by using a simple layer attenuation model including the photoionization cross sections by Scofield [40] and inelastic mean free paths for SiC [41], theoretical Si 2p/C 1s intensity ratios of 1.08 and 0.92 are calculated for SiC(0001) and SiC(000$\bar{1}$), respectively, which are in excellent agreement with the measured values. This indicates that both SiC(0001) and SiC(000$\bar{1}$) surfaces are stoichiometric, i.e. that there is no excess carbon or silicon present at the surface, which is consistent with an ideal bulk termination.

3.3.2. Characterization by SXPS. Highly resolved core level spectra of H terminated SiC{0001} surfaces were measured at the synchrotron radiation source BESSY II. The spectra were deconvoluted [41, 42] into so-called Voigt lines, which is a common technique to gain

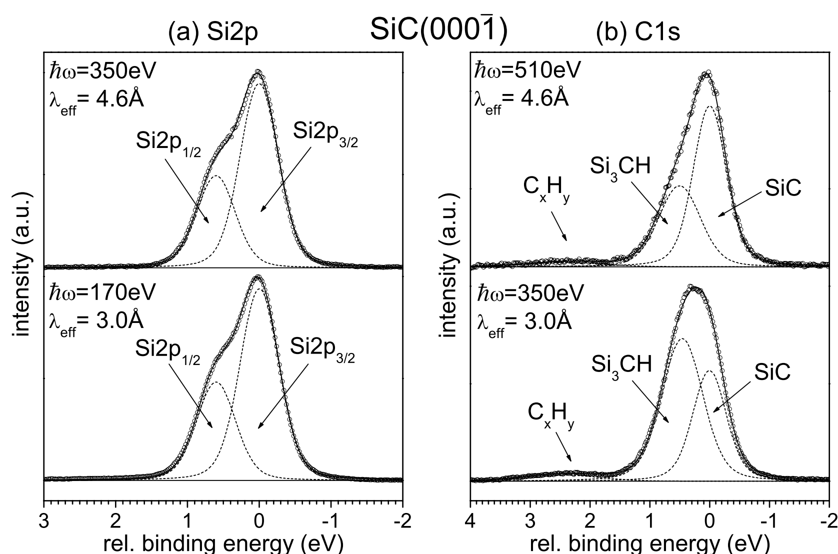

Figure 8. Highly resolved Si 2p (a) and C 1s (b) spectra of H terminated 6H-SiC(000$\bar{1}$) [41, 42]. Also shown is a deconvolution of the spectra using Voigt lines. The binding energy scale is with respect to the bulk component (SiC).

detailed information about different chemically shifted components, which may contribute to a core level spectrum. Voigt lines are a convolution of Lorentzian and Gaussian line shapes. The experimental resolution, the samples' inhomogeneity and phonon broadening contribute to the Gaussian width (ω_G) and the Lorentzian width (ω_L) is associated with the lifetime of the core hole. A so-called Shirley background [43] was subtracted from the spectra before curve fitting.

Figure 8 displays the Si 2p and C 1s core level spectra of a hydrogenated 6H-SiC(000$\bar{1}$) surface [41, 42]. Photon energies of 170 and 350 eV were applied for the measurements of the Si 2p core level, resulting in effective sampling depths of $\lambda_{eff} = 3.0$ and 4.6 Å [41], respectively. For the energetically lower lying C 1s core level the same effective sampling depths are obtained with photons of 350 and 510 eV, respectively. The Si 2p spectrum in figure 8(a) consists of a single spin–orbit split doublet due to emission from bulk SiC. The spin–orbit splitting was determined as 0.606 ± 0.003 eV and the branching ratio was 0.516 ± 0.004. In agreement with the XPS results presented in section 3.3.1, no oxygen related contributions are present in the spectrum. The C 1s spectra (figure 8(b)) are made up of three components. Two of them increase with decreasing probe depth and are therefore due to emission from the surface. The component labelled C_xH_y in figure 8(b) with a chemical shift of 2.4 eV with respect to the bulk component can be ascribed to a minute contamination with hydrocarbons, which was observed to increase with storage time of the sample in the vacuum transport chamber. A quantitative evaluation of the relative signal strength observed on the samples studied at BESSY II indicates that the hydrocarbon coverage was of the order of 2–5% of a monolayer. No such contamination was observed in our home laboratory using XPS under a take-off angle of 75°, which reduces the probe depth to 4 Å. The other surface component, which is labelled Si_3CH in figure 8(b), is due to the topmost carbon layer in which the carbon atoms are bound to three Si atoms of the same bilayer and to one hydrogen atom. The chemical shift with respect to the bulk line is 0.47 ± 0.02 eV.

Figure 9 shows the corresponding core level spectra taken from the SiC(0001) surface [41, 42]. The same photon energies were applied as for the carbon face, leading

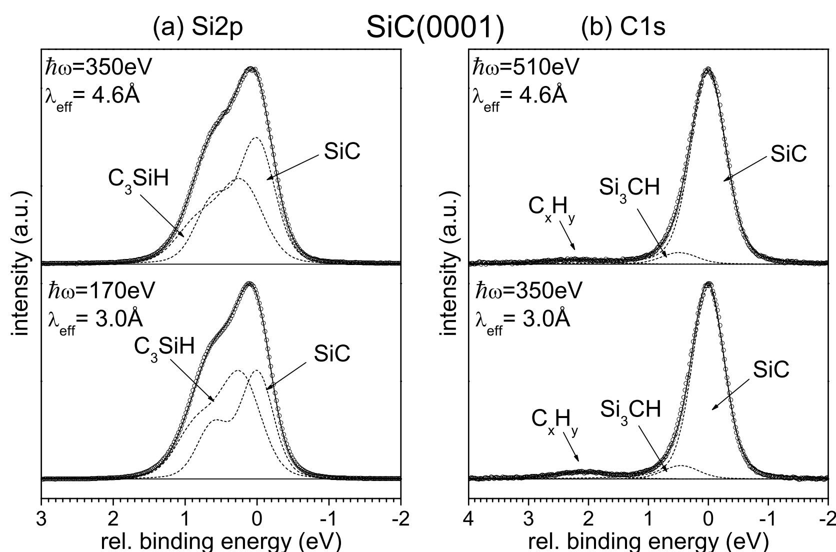

Figure 9. Highly resolved Si 2p (a) and C 1s (b) spectra of H terminated 6H-SiC(0001) together with a deconvolution obtained by a peak fit routine [41, 42]. The binding energy scale is with respect to the bulk component (SiC).

to the same effective sampling depths. The shape of the Si 2p core level in figure 9(a) indicates that the spectrum must contain at least two doublets. A chemically shifted component due to oxygen can be excluded on the basis of XPS measurements, which showed that the surfaces are oxygen free. Surprisingly, no significant dependence on the effective sampling depth is observed, which indicates that the shift of the surface component must be rather small. This again rules out oxygen as being responsible for the signal shape, because the oxygen induces a relatively large chemical shift of 0.5–0.6 eV per oxygen bond [17, 18, 44–46], which would lead to a clear photon energy dependence. Therefore we have chosen to fit one bulk component and a chemically shifted surface component due to Si atoms in a C_3SiH configuration to the spectrum. As a constraint we used the surface to bulk intensity ratios obtained from the fits of the C 1s core level spectra taken from the SiC($000\bar{1}$) surface. This procedure results in the fits also shown in figure 9(a) for the Si 2p core level. The surface component is shifted to higher binding energy by 0.22 ± 0.02 eV. However, due to the fact that the line shape is invariant to changes in the photon energy, it is also possible to get acceptable fits inverting this assignment, i.e. assuming that the surface component is located at lower binding energy. This behaviour may be a result of the intrinsically large Gaussian width of the core levels (around 0.6–0.7 eV [41]) which are in agreement with previously published results on SiC surfaces (see e.g. [10]) and (compared to the Gaussian width) the small chemical shift of only 0.22 eV. Our assignment is corroborated by comparing the binding energy difference between the bulk C 1s and Si 2p core level emission, which can be determined from bulk sensitive XPS measurements with an accuracy of 50 meV [41]. On the other hand, initial state arguments favour the opposite assignment, since hydrogen is less electronegative than carbon. Further investigations are necessary to clarify this issue.

Figure 9(b) shows the C 1s core level of the hydrogenated 6H-SiC(0001). The shape of the main contribution appears much less asymmetric when compared with the C 1s core levels of 6H-SiC($000\bar{1}$). Nevertheless, three components are needed to yield satisfactory fitting results. The intense main line can be assigned to emission from the bulk (labelled SiC). The small

surface component with a chemical shift of 2.2 ± 0.1 eV was also observed on the C face and is due to tiny amounts of hydrocarbons (C_xH_y). The third component, which is also located at the surface, has a chemical shift of 0.47 ± 0.03 eV in good agreement with the hydrogen induced surface component on 6H-SiC(000$\bar{1}$). This points to the presence of carbon atoms on the surface, which are bound to one hydrogen atom and three silicon atoms (Si_3CH). This is reasonable since epitaxial layers on off-axis cut SiC(0001) surfaces as well as polished on-axis substrate surfaces contain a significant number of steps, where carbon atoms are exposed. Considering the small hydrogen induced chemical shift of the Si 2p core level (0.22 eV, see above) it is no surprise that no such component was observed in the Si 2p spectra of the C face.

Summarizing the experimental results presented in this section we can state that the method introduced in section 2 produces 6H-SiC{0001} surfaces which are free of unwanted contamination and are stoichiometric, well ordered and hydrogen saturated. In the following sections additional properties of these surfaces will be explored.

4. Chemical stability of hydrogenated 6H-SiC{0001} surfaces

The stability of hydrogen saturated 6H-SiC(0001) surfaces against oxidation was first studied by van Elsbergen *et al* [29] using XPS. They observed that compared to the Si-rich $(\sqrt{3} \times \sqrt{3})R30°$ reconstructed surface the oxygen uptake was drastically reduced after the surface dangling bonds were saturated by atomic hydrogen, which was produced by cracking molecular hydrogen on a hot tungsten filament. Van Elsbergen *et al* [29] determined that the initial sticking coefficient for oxygen was reduced by a factor of 10^{10}. Tsuchida *et al* [16] investigated the stability of hydrogenated 6H-SiC{0001} surfaces by measuring the Si–H and C–H stretch modes after exposure of the samples to air. While the Si–H stretch mode of SiC(0001) shows a slow broadening over a period of four days, the C–H stretch mode of SiC(000$\bar{1}$) appears to vanish much faster, i.e. within 2 h. This is puzzling because the C–H bond is expected to be more stable than the Si–H bond. As an explanation it was suggested that the C–H mode is covered up by an increasing hydrocarbon contamination. That this is indeed the case will be discussed below.

The passivating effect of surface hydrogenation was also studied in our group [34, 37–39]. XPS spectra of 6H-SiC{0001} taken after the samples had been exposed to air for 2 h (see figure 10) indicated the presence of oxygen in much smaller quantities than on the wet-chemically prepared surfaces (cf figure 7). On SiC(0001), the oxygen uptake as determined by the ratio of the O 1s signal to the sum of C 1s and Si 2p intensities amounts to 1.5% after a total oxygen exposure of 3×10^{26} O_2 molecules cm^{-2}. This value is a factor of 17 lower than that achieved by van Elsbergen and co-workers [29]. The C/Si ratio was observed to increase somewhat, indicating the presence of excess carbon on the surface.

The chemical nature of the oxygen and excess carbon present after exposure to air is revealed by taking a closer look at the Si 2p and C 1s core level spectra. This is shown in figure 11 for 6H-SiC(0001) [39]. The asymmetric shape of the Si 2p spectra shown in that figure which has already been discussed in section 3.3.2 shows hardly any change with photon energy, indicating that no chemically shifted components due to silicon–oxygen bonds are present even after exposing the sample to air for 2 days. The C 1s spectra, however, show a clear surface component with a chemical shift of 2.1–2.5 eV, which is consistent with hydrocarbon contamination. Thus, the oxygen observed in XPS must be in the form of oxygen containing hydrocarbons such as alcohols and other solvents, which are frequently present in a surface science laboratory. It is clear from figure 11 that the thickness of hydrocarbon layer increases with storage time. When assuming that the density of the hydrocarbon layer is similar to that of gasoline (0.75 kg l^{-1}), the thickness of the overlayer can be estimated. In

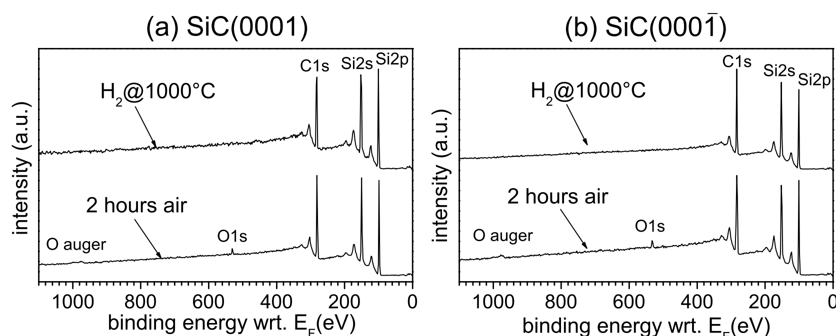

Figure 10. XPS survey scans of (a) 6H-SiC(0001) and (b) 6H-SiC(000$\bar{1}$) taken directly after hydrogenation and after exposure to air for 2 h.

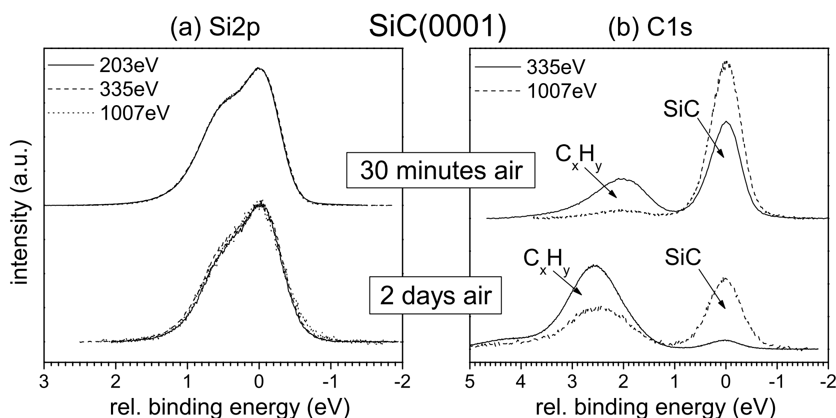

Figure 11. Highly resolved Si 2p and C 1s spectra of hydrogen passivated 6H-SiC(0001) taken after exposure to air [39].

this way we obtain an overlayer thickness of 1.5 ± 0.6 Å for the sample exposed to air for about 30 min and 9.0 ± 1.0 Å for the sample exposed to air for two days.

5. Stacking rearrangement of 6H-SiC(0001) during high-temperature hydrogen treatment

As mentioned in section 3.2, we have observed a split absorption signal of the Si–H stretch mode on H terminated 6H-SiC(0001). Such a splitting was also observed by Tsuchida and co-workers, who suggested that the splitting is due to a microscopically rough surface. This was supported by the presence of Si–H_2 and Si–H_3 modes in their FTIR-ATR spectra. However, as outlined above, our surfaces show all signs of a high degree of order. Therefore another explanation of the observed splitting is required.

As an alternative explanation we suggest [37–39] that the splitting of only 5.5 cm^{-1} is due to different third-neighbour interactions resulting from the different surface terminations discussed in section 3.1. While the terminations S2 and S3 in figure 5 have a cubic stacking directly below the surface bilayer, S1 is characterized by a hexagonal stacking configuration directly below the topmost bilayer. The third-neighbour environment of the 'cubic' terminations S3 and S2 is different from the 'hexagonal' termination S1. In the latter

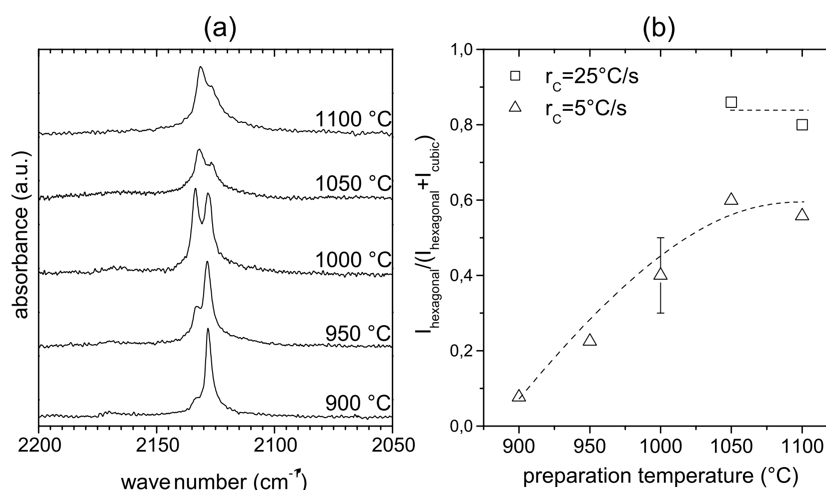

Figure 12. (a) FTIR-ATR spectra of the Si–H stretch mode on 6H-SiC(0001) taken after hydrogenation at different sample temperatures. (b) Intensity of the signal due to hexagonal S1 termination normalized to the total intensity. Values for slow ($5\,^{\circ}\mathrm{C\,s^{-1}}$) and rapid ($25\,^{\circ}\mathrm{C\,s^{-1}}$) cooling rates after hydrogenation are shown.

case the carbon atom of the second bilayer is located directly below the Si–H bond, which is not true for S3 and S2. In order to support this explanation for the split Si–H stretch mode we have performed infrared absorption measurements on hydrogenated (111) surfaces of cubic 3C-SiC [47–49]. For 3C-SiC(111) the terminations should be 'cubic' (see figure 1) and we expect to observe only one absorption line. This is indeed the case: on 3C-SiC(111) a single mode is observed at $2128.4 \pm 1.0\ \mathrm{cm^{-1}}$. In this way we were able to identify the signal at $2128.0 \pm 0.6\ \mathrm{cm^{-1}}$ on 6H-SiC(0001) as being due to cubic terminations. The other absorption line observed on 6H-SiC(0001) at $2133.5 \pm 0.6\ \mathrm{cm^{-1}}$ could not be observed on 3C-SiC(111) and must then be due to the hexagonal S1 termination.

Interestingly, we observe that the ratio of two Si–H stretch mode signals measured on 6H-SiC(0001) varies with preparation temperature. This is shown in figure 12. Whereas the spectrum of the sample prepared at 900 °C contains almost exclusively the signal assigned to cubic terminations, samples prepared at higher temperatures show an increasing absorption line due to hexagonal S1 termination. Preparation at 1050 °C leads to a saturation of the intensity of the hexagonal mode with a saturation value of about 60% of the total intensity. This saturation value can be increased to 85% by cooling the sample faster after completion of the hydrogenation process. Apparently, the surface termination changes from hexagonal to cubic during slow cooling of the sample.

For further investigation of the observed stacking rearrangement the etch rates of SiC were measured on cubic 3C-SiC films of the three different orientations, (111), (110) and (100) [47, 49]. The hydrogen induced removal of SiC ranges from $13\ \mathrm{Å\,h^{-1}}$ at 1000 °C to $100\ \mathrm{Å\,h^{-1}}$ at 1150 °C. Thereby, the etch rates turned out to be independent of the surface orientation, which supports the assumption that they are equal for 3C-SiC and 6H-SiC. Based on this assumption we estimate that during slow ($5\,^{\circ}\mathrm{C\,s^{-1}}$) and fast ($25\,^{\circ}\mathrm{C\,s^{-1}}$) cooling from 1050 to 900 °C a maximum of 5 and 1% of a bilayer is etched, respectively. Obviously, the observed change in surface termination cannot be explained by etching of SiC during slow cooling.

Instead, a phase transition is proposed, in which the 6H-SiC(0001) surface is transformed from a hexagonally terminated surface, which is stable at temperatures of 1050 °C and above,

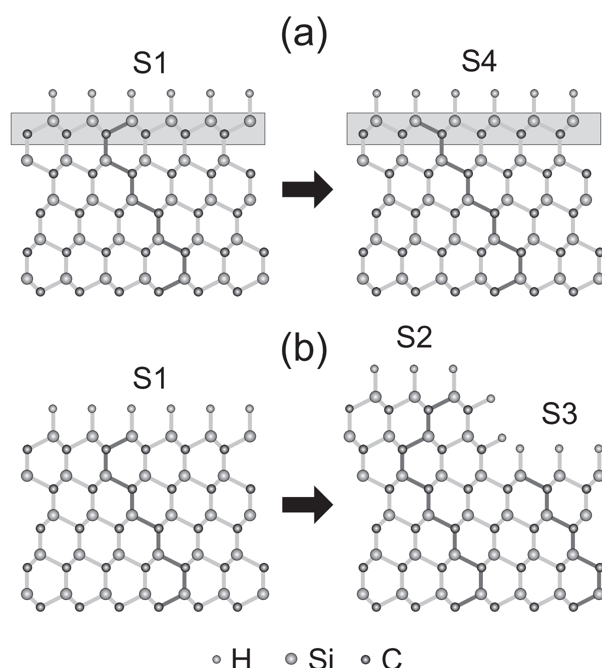

Figure 13. Possible mechanisms [49] for the stacking rearrangement observed during hydrogenation of 6H-SiC(0001): bilayer rotation (a) and lateral mass transport (b).

into a preferentially cubic terminated surface which is the stable state at lower temperatures (900 °C). The timescale on which this phase transition takes place can be estimated from the cooling rates and is of the order of a few tens of seconds. These observations agree well with a number of other experimental results reported in the literature. Kimoto *et al* [50] determined the step height distribution on homoepitaxially grown 6H-SiC films by transmission electron microscopy (TEM) and found that 88% of the steps are three bilayers high, indicating that 88% of the surface should have the same termination. Using scanning tunnelling microscopy, Starke and co-workers [9] observed step heights integer multiples of three bilayers. In addition, using the LEED-$I(E)$ technique they also determined that wet-chemically cleaned SiC(0001) surfaces contained 80% cubic termination and 20% hexagonal termination [8, 9, 51–54]. On the other hand, at a preparation temperature of 1050 °C and higher, the hexagonal termination is preferred, which is in agreement with the fact that hexagonal polytypes like 4H- and 6H-SiC are preferably grown at higher temperatures than cubic 3C-SiC [50, 55–57].

The exact atomic mechanism of the stacking rearrangement is unclear as yet. It may occur via lateral mass transport or by bilayer rotation, as shown in figure 13. The term bilayer rotation does not of course mean that a whole bilayer is rotated. It is sufficient to change the bond configuration by 60°. This process may start at the edge of a terrace. Further experiments are needed in order to identify the mechanism. A structural study using the LEED-$I(E)$ technique could identify which cubic termination (S2, S3 or even S4) is present. Lateral mass transport would most likely lead to a S2/S3 terminated surface (see figure 13), while a bilayer rotation would result in a S4 terminated surface. We have to note, however, that massive lateral mass transport beyond the picture shown in figure 13 could also take place. A similar stacking rearrangement is observed in the case of the Si-rich $(\sqrt{3} \times \sqrt{3})$R30° reconstruction on 4H-SiC(0001) [58]. There the preferred termination is S3 (65%) for Si-rich preparation conditions

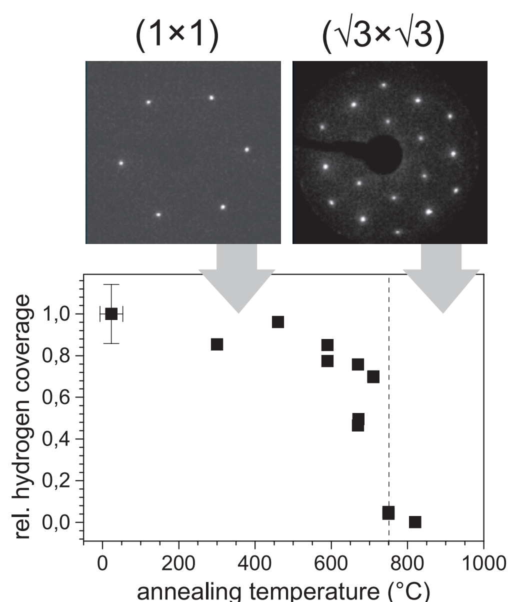

Figure 14. Hydrogen coverage as determined from the intensity of the Si–H stretch mode signal as a function of annealing temperature [41]. Also shown are representative (1×1) and $(\sqrt{3} \times \sqrt{3})$R30° LEED patterns taken before and after completion of thermal hydrogen desorption.

and S2 (75%) for Si-poor preparation conditions. Based on large morphological changes during the stacking transformation which were observed using STM, the authors favour a mechanism involving extensive lateral mass transport.

6. Reconstructions of 6H-SiC{0001} after thermal hydrogen desorption

Annealing the hydrogen saturated 6H-SiC{0001} surfaces to elevated temperatures in UHV leads to the desorption of hydrogen and the formation of reconstructions [37, 38, 41]. On the Si face the desorption of hydrogen starts at a temperature just above 700 °C as witnessed by the reduction of the intensity of the Si–H stretch mode in FTIR-ATR (cf figure 14). The desorption of hydrogen is accompanied by the transformation of the (1×1) LEED pattern to a $(\sqrt{3} \times \sqrt{3})$R30° diffraction image. The transformation is completed at an annealing temperature of 820 °C.

Si 2p and C 1s core level spectra of SiC(0001)-(1×1)-H taken after successive annealing steps show only marginal changes up to an annealing temperature of 640 °C. These slight variations can be explained by a partial desorption and decomposition of residual hydrocarbon contamination [41]. Significant changes occur between 640 and 820 °C. Figure 15(a) shows a Si 2p spectrum of 6H-SiC(0001) taken after thermal hydrogen desorption and conversion to the $(\sqrt{3} \times \sqrt{3})$R30° structure [41]. The spectrum can be deconvoluted into one bulk component and two surface components labelled $S_{Si}1$ and $S_{Si}2$ with chemical shifts of -1.10 ± 0.06 and -0.33 ± 0.04 eV with respect to the SiC bulk component. This observation is in good agreement with the SXPS study of the Si-rich $(\sqrt{3} \times \sqrt{3})$R30° reconstruction by Johansson *et al* [10], who prepared this reconstruction by annealing wet-chemically treated SiC(0001) at 950 °C in UHV, and the XPS study of Tautz *et al* [30]. In the latter work the $(\sqrt{3} \times \sqrt{3})$R30° reconstruction was formed by annealing the Si-rich (3×3) phase at 950 °C for several minutes.

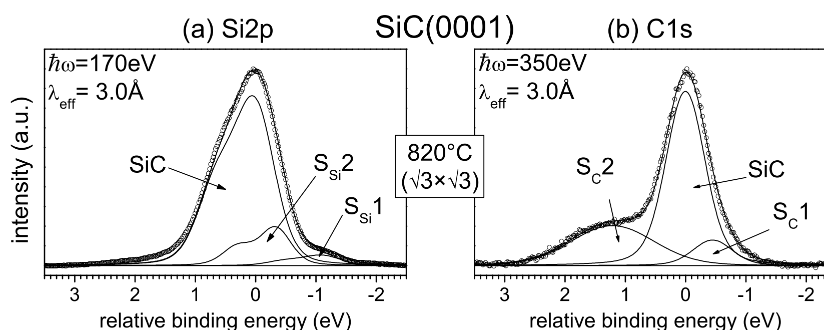

Figure 15. (a) Si 2p and (b) C 1s spectra of 6H-SiC(0001) taken after thermal hydrogen desorption [41]. Also shown is a deconvolution into bulk and surface components. The binding energy is given with respect to the bulk component.

The atomic structure of this reconstruction was determined by a dynamical LEED study [58]. The surface component $S_{Si}2$ at -0.33 eV is due to the Si atoms of the topmost SiC bilayer for which the more electronegative binding partner carbon is replaced by Si adatoms. These adatoms which give rise to the second chemically shifted component ($S_{Si}1$) are situated in so-called T_4 sites. Each of them is bound to three Si atoms of the topmost SiC bilayer, thus forming the $(\sqrt{3} \times \sqrt{3})$R30° super structure. We also find that the fit in figure 15 is not perfect at the higher binding energy side. There a weak tailing is observed which indicates the onset of oxidation of this highly reactive surface [59].

The C 1s spectrum of the same surface shown in figure 15(b) is made up of three components as well [41], in agreement with the observations of Johansson *et al* [10]. Two surface components S_C1 and S_C2 are located at binding energies of -0.43 ± 0.07 and 1.20 ± 0.10 eV relative to the bulk component, respectively. The component S_C1 is due to the carbon atoms of the topmost bilayer [10]. At the silicon-rich surface the effective electronegativity of all interface silicon atoms appears reduced, which causes a very small chemical shift to lower binding energy of the component due to the next neighbouring carbon atoms. The second surface component S_C2 has been subject to a lively discussion [10, 30, 41]. Johansson *et al* [10] discussed explanations for S_C2 which were incompatible with the structural model established by a later LEED-$I(E)$ study [58]. Tautz *et al* [30], who prepared the $(\sqrt{3} \times \sqrt{3})$R30° structure by annealing the SiC(0001) surface in a flux of silicon, suggested that the component S_C2 is due to contamination from the residual gas. This was based on the observation of a time dependent increase of the S_C2 signal. However, it has to be distinguished how the $(\sqrt{3} \times \sqrt{3})$R30° reconstruction is formed. When forming the adatom structure by annealing (1×1) phases without Si flux the adatoms must come from an internal source. Therefore our explanation for the S_C2 observed by us [41] and Johansson [10] is that it is due to a disproportionation of SiC which is necessary to yield the Si atoms for the formation of the adatom structure [41]. The (1×1) surfaces, which are initially stoichiometric in our case, decompose partly, leading to mobile Si atoms which diffuse along the surface and eventually form the $(\sqrt{3} \times \sqrt{3})$R30° structure. Simultaneously, carbon-rich areas are formed as an intrinsic by-product. The method employed by Tautz *et al* [30] provides an external source for the Si adatoms. Therefore their S_C2 component must be of extrinsic nature, which is supported by the observed time dependence. The above arguments are corroborated by a recent work of Virojanadara and Johansson [46], who were able to prepare the $(\sqrt{3} \times \sqrt{3})$R30° phase by annealing the oxidized 4H-SiC(0001) surface at 1120 °C. In this case the oxide layer constitutes the external source for the Si adatoms and the formation of S_C2 is completely suppressed.

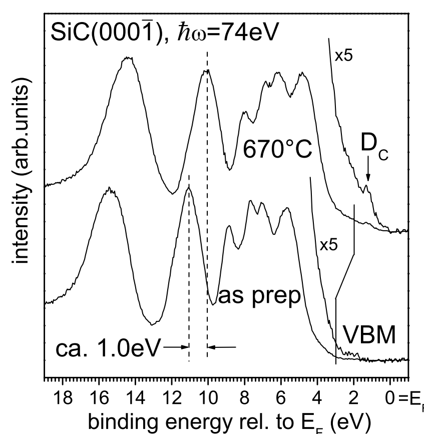

Figure 16. Valence band spectra of hydrogenated 6H-SiC(000$\bar{1}$) directly after preparation and after annealing in UHV to 670 °C [41]. The binding energy is given with respect to the Fermi level (E_F).

Interestingly, the temperature at which the $(\sqrt{3} \times \sqrt{3})$R30° structure develops from hydrogenated SiC(0001) is 750 °C. The other preparation methods require higher temperatures (>900 °C) [10, 30, 46]. Although a direct comparison of published temperature values is difficult due to possible differences in the temperature calibration, it appears that the lower temperature observed on the hydrogenated surface may be due to the lower temperature necessary for hydrogen desorption as compared with the desorption temperature of oxygen and silicon. It is also obvious that the same temperature yields the activation energy for the formation of the $(\sqrt{3} \times \sqrt{3})$R30° reconstruction by the mechanism discussed above.

Similar desorption experiments to the ones described above were also carried out with the hydrogen terminated SiC(000$\bar{1}$) surface [41]. In this case no changes in the core level spectra were observed up to a temperature of 820 °C, with the only exception being a partial desorption of the minute hydrocarbon contamination discussed in section 3.3.2. In addition, the (1×1) diffraction pattern remained visible up to 820 °C. However, hydrogen desorption already starts after heating the sample to 670 °C as indicated by the formation of a db surface state above the VBM. This is shown in figure 16. A similar db state has previously been observed on the silicate adlayer reconstruction on 6H-SiC(000$\bar{1}$) [24]. In contrast to the case of the Si face (see above) thermal hydrogen desorption apparently commences without the immediate formation of a surface reconstruction. This behaviour may be due to a stronger localization of the carbon valence orbitals which would cause unfavourable bond angles and lengths on reconstructed surfaces [60].

Further heating of the 6H-SiC(000$\bar{1}$) sample to 950 °C transforms the LEED pattern from (1×1) to (3×3) [41], an observation which was previously reported by several other groups [19, 61, 62]. Corresponding Si 2p and C 1s core level spectra are depicted in figure 17. The C 1s core level spectrum (see figure 17(b)) can be fitted using three components. One component (SiC) is due to emission from the bulk; the other two components (S_C1 and S_C2) are due to surface carbon atoms [41]. The variation of the relative intensities of these two surface components with photon energy and thus probe depth suggests that the C atoms corresponding to S_C1 are located above the C atoms corresponding to S_C2. The latter are located above the carbon atoms of the bulk. These intensity variations are in contrast to the results presented by Johansson *et al* [19], who observed the inverse behaviour. In their case, however, a much larger Gaussian width of $\omega_G = 2.1$ eV was required for component S_C1. In

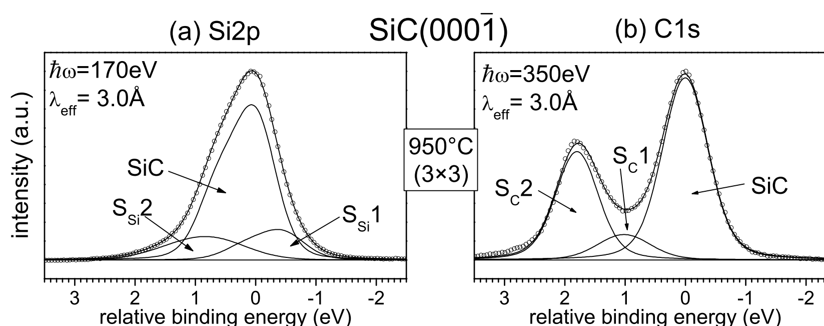

Figure 17. (a) Si 2p and (b) C 1s spectra of 6H-SiC(000$\bar{1}$)-(3 × 3) prepared by annealing the hydrogen terminated surface at 950 °C [41]. Also shown is a deconvolution into bulk and surface components. The binding energy is given with respect to the bulk component.

our case, $\omega_G = 0.9 \pm 0.07$ eV, which is only slightly larger (0.2 eV) than the Gaussian widths of the other two components, leads to satisfactory curve fits. The origin of this discrepancy is unclear. One may speculate, however, that it is due to the initially larger hydrocarbon contamination present on the wet-chemically cleaned surfaces used in their study. Based on our spectral data we propose [41] that the (3 × 3) structure consists of carbon adatoms on top of a carbon interface layer. The intensity ratio of S_C1 to S_C2 is around 0.3, which suggests that one carbon atom corresponding to S_C1 is situated above three to four carbon atoms corresponding to S_C2. Nevertheless, proposing a more detailed structural model based on the data at hand would be too speculative.

The Si 2p core level (see figure 17(a)) shows two chemically shifted surface components as well [41]. Component $S_{Si}1$ suggests the presence of excess Si which is formed in a way equivalent to the excess carbon observed on the Si face discussed above, i.e. disproportionation of SiC. The second surface component, $S_{Si}2$, is located at 0.63 eV higher binding energy, which indicates the onset of oxidation of the Si enriched regions and formation of Si^+. In contrast to our spectra, Johansson *et al* [19] did not observe any surface components in their Si 2p spectra. The reason for this discrepancy may be the initial hydrocarbon contamination on the wet-chemically prepared samples, which may yield at least part of the carbon necessary for the (3 × 3) structure without disproportionation of SiC.

7. Electronic properties of unreconstructed 6H-SiC{0001} surfaces

During our studies of hydrogenated 6H-SiC{0001} surfaces we observed that a high flux of synchrotron radiation leads to the desorption of hydrogen as well [42]. The advantage of this 'cold' desorption is that it apparently does not provide the necessary activation energy for reconstruction. As a consequence, the surfaces retain their (1 × 1) periodicity. This was observed by LEED as well as in the core level spectra, which are displayed in figure 18(a). As can be seen from that figure, the line shape of the Si 2p core level remains unaffected during the first two periods of irradiation. Only a minute reduction of the signal width is recognizable. In addition, only the spectrum taken after the third and final period of irradiation shows a slight tailing at the high-binding-energy side. This indicates the onset of oxidation of the hydrogen-free and hence highly reactive surface. Surface components due to the $(\sqrt{3} \times \sqrt{3})$R30° structure are absent.

The reason for the high reactivity of the irradiated surfaces is the formation of dangling bonds which can be observed by the appearance of a surface state 0.6 eV above the VBM

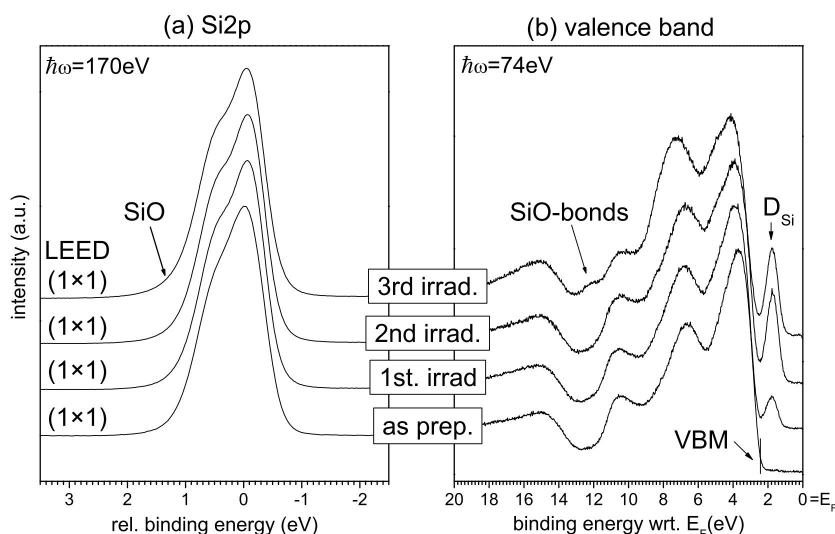

Figure 18. (a) Si 2p and spectra of 6H-SiC(0001) taken after photon induced desorption of hydrogen. (b) Corresponding valence band spectra.

within the fundamental bandgap of SiC. This is demonstrated in figure 18(b), where valence band spectra are shown, which were taken under the same conditions as the Si 2p spectra in figure 18(a). The db state which is labelled D_{Si} in figure 18(b) reaches saturation after the second period of irradiation. In addition, a small signal due to Si–O bonds within the ionic gap of SiC [24, 25] shows up after the third irradiation, in agreement with the Si 2p spectra discussed above.

To our knowledge, this is the first time that clean and unreconstructed SiC{0001} surfaces have been prepared. It is interesting to note that the db state is located at a binding energy of 1.78 ± 0.05 eV, well below the Fermi level. A similar behaviour was reported for the carbon face [34, 42]. In this case a db state was measured at a binding energy of 1.9 eV below the Fermi level [34]. The surfaces thus show a semiconducting behaviour rather than the expected metallic behaviour which is predicted within the single-particle picture [60, 63].

Similar db states were previously observed on 6H-SiC($000\bar{1}$) with silicate adlayer reconstruction [24, 25], on the $(\sqrt{3} \times \sqrt{3})$R30° reconstructed SiC(0001) surface [64] and on 3C-SiC(111) with the Si-rich (3×3) reconstruction [65]. In all cases the db states were observed below the Fermi level, which is indicative of a semiconducting character of the surface. In order to account for the semiconducting behaviour, a description beyond the single-particle picture is necessary. Such a model is the Mott–Hubbard metal–insulator transition [66–69] which occurs when the correlation energy U which is necessary to put a second electron into an already half filled db state is larger than the band width B. The latter is directly correlated with the interaction strength (and thus distance) of neighbouring db states. As a result, a splitting into a filled lower and an unfilled upper Hubbard band takes place as shown in figure 19 for an n-type surface. These are separated by the correlation energy U and are characterized by the band widths B_{l} and B_{u}, respectively. On an n-type surface the upper Hubbard band will be partially occupied by electrons from donors near the surface. The surface Fermi level will then be pinned (see also section 8) at the lower edge of the upper Hubbard band. A more detailed presentation of correlation effects on semiconductor surfaces in general and on SiC surfaces in particular can be found in a review by Flores *et al* [70] and in the article by Bechstedt in the present volume, respectively.

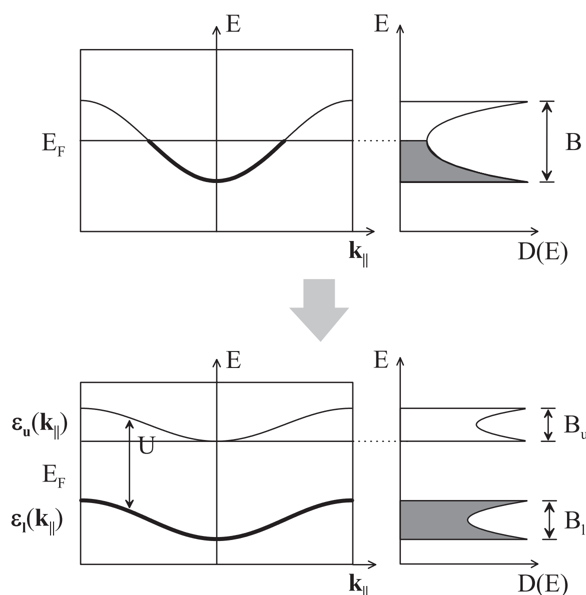

Figure 19. Schematic representation of the Mott–Hubbard metal–insulator transition on an n-type surface.

The observation of the db states below E_F suggests that the bandwidth B of the db bands must be smaller than the correlation energy U. In our experiment, the binding energies of D_{Si} and D_C are 1.78 ± 0.05 and 1.9 ± 0.1 eV [34, 42], respectively, which can be taken as lower limits for the Hubbard U, assuming that this model applies in our case. Indeed, the band width B calculated by density functional theory using the local density approximation (DFT-LDA) [60] is of the order of 1 eV for SiC(0001) and 0.3 eV for SiC(000$\bar{1}$), respectively. The latter value is smaller due to a stronger localization of the carbon db as compared to the silicon db. The Hubbard U calculated for the $(\sqrt{3} \times \sqrt{3})$R30° structure of 6H-SiC(0001) is 1.95 eV [71]. We also note that calculations by another group yield a similar result of 2.1 eV for 3C-SiC(111)-$(\sqrt{3} \times \sqrt{3})$R30° [72], but a smaller value of 1.0 eV for the Si-rich 3C-SiC(111)-(3×3) reconstruction. The difference is due to different screening on the two surfaces. Thus for 6H-SiC(0001)-(1×1) a similar or slightly larger U than for the $(\sqrt{3} \times \sqrt{3})$R30° structure is expected. Corresponding calculations for the (1×1) surfaces are not available in the literature. The dispersion of the db states observed on hydrogen-free SiC(0001) and SiC(000$\bar{1}$) is the subject of ongoing investigations.

8. Electronic passivation of 6H-SiC{0001} surfaces by dangling bond saturation with hydrogen

Figure 20 depicts XPS spectra of the C 1s and Si 2p core levels of p-6H-SiC(0001) and n-type 6H-SiC(000$\bar{1}$) taken after wet-chemical cleaning and after hydrogenation. The binding energies are given with respect to the Fermi level. Following hydrogenation, contributions to the signals due to oxygen and hydrocarbon contaminations are removed, leading to C 1s and Si 2p spectra as discussed above. Both core levels of the p-type 6H-SiC(0001) sample are shifted to lower binding energy, indicating a change in surface band bending such that the surface Fermi level moves closer to the VBM. The vertical lines indicate the positions of

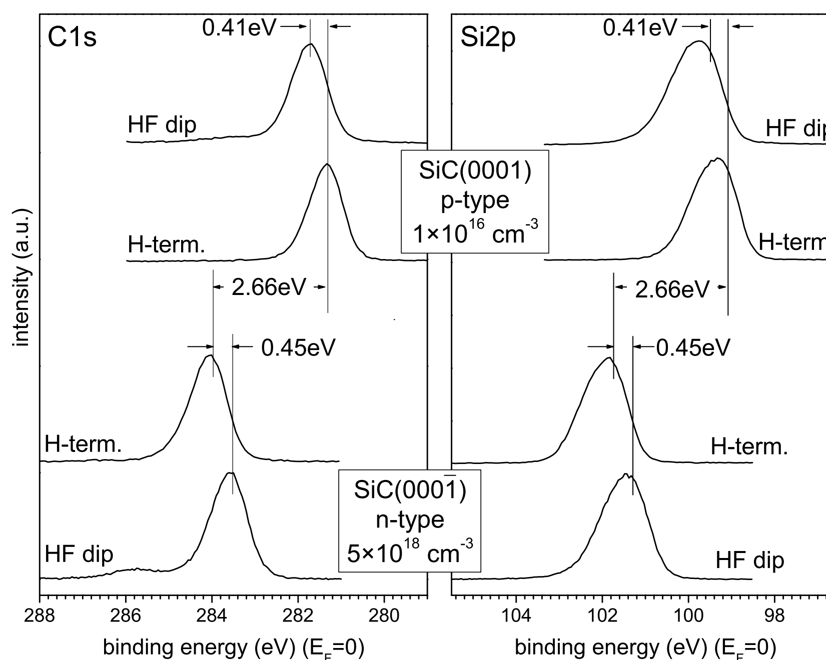

Figure 20. XPS spectra of the C 1s (left) and Si 2p (right) core levels of p-type 6H-SiC(0001) (upper spectra) and n-type 6H-SiC(000$\bar{1}$) (lower spectra) taken after wet-chemical cleaning and after hydrogenation. Binding energies are given with respect to the Fermi level. The vertical lines indicate the C 1s and Si $2p_{3/2}$ bulk binding energies obtained by a peak fit.

the bulk C 1s and Si 2p core levels, which shift together by −0.41 eV. On the n-type sample, however, the opposite behaviour is observed. In this case the common shift is +0.45 eV. The maximum difference in binding energies observed on p- and n-type samples is 2.66 ± 0.05 eV.

The reason for the change in band bending [73] described above is a depinning of the surface Fermi level due to hydrogenation. This is depicted in figure 21 for the case of the p-type SiC(0001) surface. Before hydrogenation the surfaces contain defects and adsorbate states within the fundamental bandgap. On a p-type substrate, these partially filled surface states of amphoteric character will donate electrons towards the surface as long as they lie energetically above E_F thus creating a negative space charge, which in turn will lead to a downward band bending as shown in figure 21 for p-type SiC(0001). By analogy, on an n-type substrate (not shown in figure 21) a donation of electrons from the conduction band into the partly empty surface states occurs, leaving behind a positive space charge due to ionized donors. In this case a band bending in the opposite direction is observed. That the surface states indeed posses amphoteric character can be derived from the observation of a surface Fermi level pinning closer to midgap position on both p-type and n-type surfaces. When the surface is properly hydrogenated the adsorbate states and defect states will be replaced by Si–H bonding and antibonding states which lie in the valence or conduction band, respectively (see below). They are thus effectively removed from the gap and are no longer able to pin E_F (flat band situation).

Since the band bending shifts the band edges as well as the core levels (see figure 21), the band bending and thus the position of the Fermi level within the bandgap can be determined from the C 1s binding energy when its energetic distance to the VBM is known. Using XPS [34] this energy was measured as 281.0 ± 0.1 eV. The experimentally determined positions of the

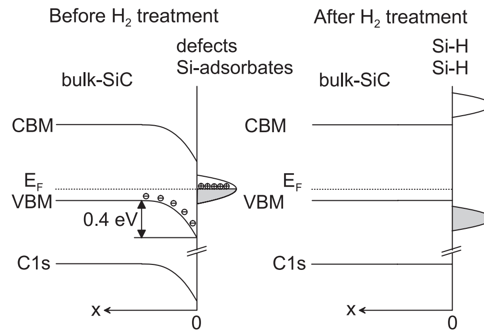

Figure 21. Band diagram of p-type SiC(0001). Before hydrogenation the surface Fermi level is pinned by adsorbate states and surface defect states within the gap. After hydrogenation all states are removed from the gap, leading to flat bands. $x = 0$ corresponds to the surface. Occupied states are indicated by cross hatching.

surface Fermi levels of different samples are shown in figure 22, where they are compared to the calculated [74] bulk values. As can be seen from that figure, flat bands are achieved for n-type 6H-SiC(000$\bar{1}$) and for p-type 6H-SiC(0001) after hydrogenation, demonstrating that hydrogenation does not only provide a chemical but also an electronic passivation of the surfaces. The experimental observation of the flat band condition indicates that bonding and antibonding C/Si–H states are located below and above the valence band and conduction band edge, respectively, where they are electrically inactive. From H terminated Si(111) [4] it is known that the bonding Si–H states are located 4.5–5.0 eV below the VBM. On the other hand, theoretical studies [75, 76] indicate that the antibonding states are located only slightly above the conduction band minimum (CBM). If we assume that they are located 0.5 eV above the CBM, we estimate a energetic difference of 6.0–6.5 eV between the bonding and antibonding Si–H states. On 3C-SiC(100)-(2 × 1)-H a hydrogen related surface state is observed at approximately 2.4 eV below the VBM [77]. Since the valence band offset between different SiC polytypes is basically zero [78], we estimate that the Si–H antibonding states on H terminated SiC(0001) are approximately 0.5–1.0 eV above the CBM.

The surface charge density q_s is related to the observed band bending $|e\phi|$ through [73]

$$q_s = \pm\sqrt{2\epsilon_0\epsilon N_{A,D}^{eff}|e\phi|}, \tag{1}$$

where ϵ_0 is the permittivity of free space, $\epsilon = 10.3$ the dielectric constant of SiC [79] and $N_{A,D}^{eff}$ the effective density of acceptors or donors, respectively. Assuming a residual bend bending of 0.05 eV which is the uncertainty in the C 1s binding energy, we estimate as upper limits for the density of surface charges 7.5×10^{10} cm^{-2} on our p-type 6H-SiC(0001) and 2.5×10^{11} cm^{-2} on n-type 6H-SiC(000$\bar{1}$) [37–39]. Slight annealing of the electronically passivated samples in UHV immediately induces a band bending (see figure 22). This is most likely due to partial desorption of hydrogen in such small amounts that it cannot be detected with our spectroscopic methods.

Interestingly, we have so far failed to achieve flat bands on n-type 6H-SiC(0001) (cf figure 22), whereas there is no problem in creating an electronically passivated p-type 6H-SiC(0001) surface. What is the reason for this behaviour? One possible explanation is a partial desorption of hydrogen on the n-type sample. The residual band bending present on the hydrogenated n-type 6H-SiC(0001) is around 0.6 eV, which can be accomplished by a surface charge of 3×10^{12} cm^{-2}. With 1.2×10^{15} atoms cm^{-2} this implies 0.2% of a monolayer, which is likely to go undetected by our spectroscopic techniques. If this is truly the case, then the

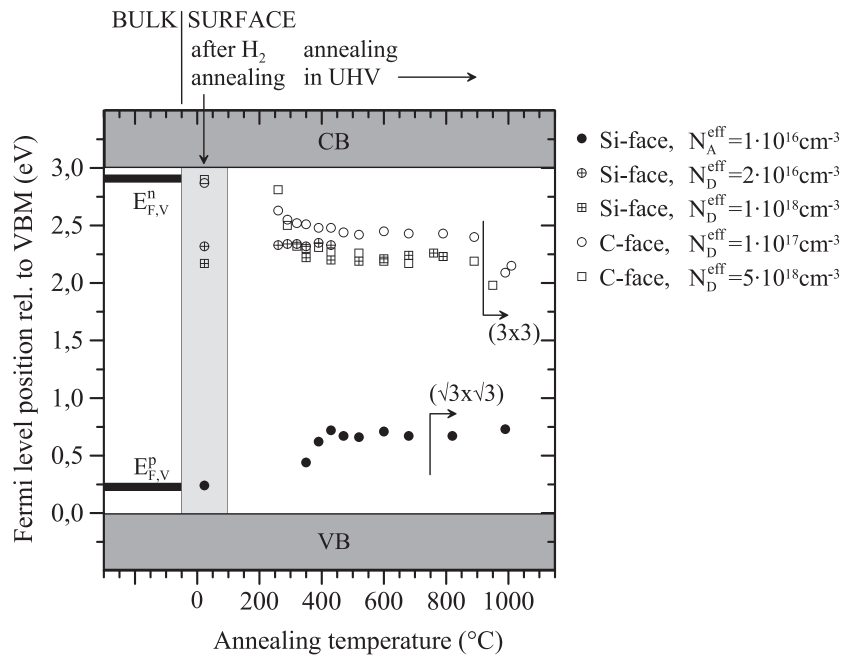

Figure 22. Surface Fermi level positions determined for a variety of 6H-SiC{0001} samples after thermal hydrogenation and after subsequent annealing in UHV in comparison with the bulk Fermi levels $E^{\mathrm{n}}_{\mathrm{F,V}}$ and $E^{\mathrm{p}}_{\mathrm{F,V}}$. The grey shaded areas indicate the valence and conduction bands, respectively. The formation temperatures of the $(\sqrt{3} \times \sqrt{3})$R30° structure on the Si face and of the (3 × 3) reconstruction on the C face are indicated as well.

question arises of why this occurs on n-type surfaces and not on p-type surfaces. The reason for this may be that on an n-type surface the electrons in the conduction band can more easily occupy the antibonding Si–H state, thus weakening the Si–H bond and enabling hydrogen desorption in small amounts. According to figure 22 the Fermi level of hydrogenated n-type 6H-SiC(0001) is pinned at 2.3 eV above the VBM. The db state which was interpreted in terms of a lower Hubbard state was observed at 0.6 eV above the VBM (see section 7). With the lower limit of the Hubbard U being 1.8 eV, the electronic states responsible for pinning of the Fermi level may thus be identical with the upper Hubbard states. The above discussion makes clear that a detailed study of the electronic structure of hydrogen-free SiC{0001} surfaces is called for.

It deserves to be mentioned that wet-chemical hydrogenation of Si(111) by buffered HF induces a superficial passivation of dopant atoms [4], thus creating an intrinsic layer at the surface. As a consequence, the surface Fermi level is observed near midgap despite an effective removal of surface and defect states. However, the dopants can be reactivated by slight annealing at 350 °C with the result that the surface Fermi level becomes unpinned. The observation of flat bands on n-type 6H-SiC(000$\bar{1}$) discussed above indicates that such a dopant passivation does not occur in SiC after hydrogenation by annealing in hydrogen.

9. Summary and outlook

In the present paper the current knowledge about hydrogen passivation of hexagonal SiC surfaces was summarized. Hydrogenation is achieved by annealing in ultra-pure hydrogen at

temperatures around 1000 °C. The surfaces prepared in this way are clean, stoichiometric, unreconstructed and chemically inert. In addition, an electronic passivation was observed on n-type 6H-SiC(000$\bar{1}$) and p-type 6H-SiC(0001). Infrared absorption measurements on 6H-SiC(0001) indicate a stacking rearrangement during thermal hydrogenation. Thermal desorption of hydrogen was studied, leading to new insights about the formation of reconstructed SiC{0001} surfaces. The preparation of hydrogen-free SiC{0001} surfaces with (1×1) periodicity and one db per unit cell has been accomplished by photo-induced hydrogen desorption. These surfaces show indications for a Mott–Hubbard metal–insulator transition.

The properties of hydrogenated SiC surfaces are certainly of great fundamental interest and will be subject to future investigations. However, it is at least of equal importance to explore the potential of surface hydrogenation of SiC as a processing step for device fabrication. This task has recently been started in our group.

Commercially available SiC devices are currently limited to Schottky diodes and the commercialization of a JFET is in sight. Ultimately, it would be an advantage if SiC could be used in power MOSFETs. Unfortunately, this is currently not possible because of the high density of electrically active interface states which are present at the SiC/SiO_2 interface (see the article by Afanas'ev *et al* in the present volume). Whereas some groups intend to improve this interface, we have recently started to investigate Al_2O_3 as an alternative gate oxide on SiC. The interface between SiC(0001) and ultra-thin Al_2O_3 layers grown by atomic layer CVD was investigated using SXPS [80]. The Si 2p spectra indicate an atomically sharp interface. First electrical measurements show that the density of interface states on hydrogenated substrates is lower than on wet-chemically treated substrates. In addition, a significantly lower density of interface states than for thermal SiO_2 gate oxides was observed [80].

Acknowledgments

Part of the work presented above was supported by the Deutsche Forschungsgemeinschaft through Sonderforschungsbereich 292 and by the Bundesministerium für Bildung und Forschung (contract number 05 SE8 WEA0). The support by the team of BESSY II is highly appreciated. Finally, fruitful discussions with Dr H Tsuchida and Dr I Kamata, as well as with Dr U Starke, are acknowledged.

References

[1] Kern W (ed) 1993 *Handbook of Semiconductor Wafer Cleaning Technology, Electronic Materials and Process Technology* (Park Ridge: Noyes)
[2] Higashi G S, Chabal Y J, Trucks G W and Raghavachari K 1990 *Appl. Phys. Lett.* **56** 656
[3] Yablonovitch E, Allara D L, Chang C C, Gmitter T and Bright T B 1986 *Phys. Rev. Lett.* **57** 249
[4] Miyazaki S, Schäfer J, Ristein J and Ley L 1996 *Appl. Phys. Lett.* **68** 1247
[5] Gräf D, Grundner M, Schulz R and Mühlhoff L 1990 *J. Appl. Phys.* **68** 5156
[6] Nakanishi S, Tokutaka H, Nishimori K, Kishida S and Ishihara N 1989 *Appl. Surf. Sci.* **41** 44
[7] Owman F and Martensson P 1995 *Surf. Sci.* **330** L639
[8] Schardt J, Brahm C, Müller S, Starke U, Heinz K and Müller K 1995 *Surf. Sci.* **337** 232
[9] Starke U, Bram C, Steiner P R, Hartner W, Hammer L, Heinz K and Müller K 1995 *Appl. Surf. Sci.* **89** 175
[10] Johansson L I, Owman F and Martensson P 1996 *Phys. Rev.* B **53** 13793
[11] Johansson L I, Owman F, Martensson P, Persson C and Lindefelt U 1996 *Phys. Rev.* B **53** 13803
[12] Elsbergen V V, Kampen T and Mönch W 1996 *Surf. Sci.* **365** 443
[13] Tsuchida H, Kamata I and Izumi K 1997 *Appl. Phys. Lett.* **70** 3072
[14] Tsuchida H, Kamata I and Izumi K 1997 *Japan. J. Appl. Phys.* **36** L699
[15] Tsuchida H, Kamata I and Izumi K 1998 *Mater. Sci. Forum* **264–268** 351
[16] Tsuchida H, Kamata I and Izumi K 1999 *J. Appl. Phys.* **85** 3569

[17] Sieber N, Seyller Th, Graupner R, Ley L, Mikalo R, Hoffmann P, Batchelor D R and Schmeißer D 2001 *Appl. Surf. Sci.* **184** 280
[18] Sieber N, Seyller Th, Graupner R, Ley L, Mikalo R, Hoffmann P, Batchelor D and Schmeißer D 2002 *Mater. Sci. Forum* **389–393** 717
[19] Johansson L I, Glans P A and Hellgren N 1998 *Surf. Sci.* **405** 288
[20] Thoms B D, Owens M S, Butler J E and Spiro C 1994 *Appl. Phys. Lett.* **65** 2957
[21] Küttel O M, Diederich L, Schaller E, Carnal O and Schlapbach L 1995 *Surf. Sci.* **337** L812
[22] Bernhardt J, Schardt J, Starke U and Heinz K 1999 *Appl. Phys. Lett.* **74** 1084
[23] Starke U, Schardt J, Bernhardt J and Heinz K 1999 *J. Vac. Sci. Technol.* A **17** 1688
[24] Hollering M, Maier F, Sieber N, Stammler M, Ristein J, Ley L, Stampfl A P J, Riley J D, Leckey R C G, Leisenberger F P and Netzer F P 1999 *Surf. Sci.* **442** 531
[25] Hollering M, Sieber N, Ristein J, Ley L, Riley J D, Leckey R C G, Leisenberger F P and Netzer F P 2000 *Mater. Sci. Forum* **338–342** 387
[26] Sieber N, Hollering M, Ristein J and Ley L 2000 *Mater. Sci. Forum* **338–342** 391
[27] Lu W, Krüger P and Pollmann J 2000 *Phys. Rev.* B **61** 13737
[28] Lu W C, Krüger P and Pollmann J 2000 *Mater. Sci. Forum* **338–342** 349
[29] Van Elsbergen V, Janzén E and Mönch W 1997 *Mater. Sci. Eng.* B **46** 366
[30] Tautz F S, Sloboshanin S, Starke U and Schaefer J A 2000 *Surf. Sci.* **470** L25
[31] Stoldt C R, Carraro C and Maboudian R 2000 *Surf. Sci.* **466** 66
[32] Hallin C, Bakin A S, Owman F, Mårtensson P, Kordina O and Janzén E 1996 *Inst. Phys. Conf. Ser.* **142** 613
[33] Owman F, Hallin C, Mårtensson P and Janzén E 1996 *J. Cryst. Growth* **167** 391
[34] Sieber N 2002 Wasserstoff- und sauerstoffstabilisierte 6H-SiC{0001}-Oberflächen—eine Studie chemischer, struktureller und elektronischer Eigenschaften *PhD Thesis* University of Erlangen Nürnberg
[35] Chabal Y and Raghavachari K 2002 *Surf. Sci.* **502/503** 41
[36] Sieber N, Seyller Th and Ley L, unpublished
[37] Sieber N, Seyller Th, Mantel B F, Ristein J and Ley L 2001 *Mater. Sci. Forum* **353–356** 223
[38] Sieber N, Mantel B F, Seyller Th, Ristein J and Ley L 2001 *Diamond Relat. Mater.* **10** 1291
[39] Sieber N, Mantel B F, Seyller Th, Ristein J, Ley L, Heller T, Batchelor D R and Schmeißer D 2001 *Appl. Phys. Lett.* **78** 1216
[40] Scofield J H 1976 *J. Electron Spectrosc. Relat. Phenom.* **8** 129
[41] Sieber N, Seyller Th, Ley L, James D, Riley J, Leckey R and Polcik M 2003 *Phys. Rev.* B **67** 205304
[42] Sieber N, Seyller Th, Ley L, Polcik M, James D, Riley J D and Leckey R G C 2002 *Mater. Sci. Forum* **389–393** 713
[43] Shirley D 1972 *Phys. Rev.* B **5** 4079
[44] Virojanadara C and Johansson L 2001 *Surf. Sci.* **472** L145
[45] Virojanadara C and Johansson L 2002 *Mater. Sci. Forum* **389–393** 701
[46] Virojanadara C and Johansson L 2002 *Surf. Sci.* **505** 358
[47] Sieber N, Stark T, Seyller Th, Ley L, Zorman C and Mereghany M 2002 *Appl. Phys. Lett.* **80** 4726
[48] Sieber N, Stark T, Seyller Th, Ley L, Zorman C and Mereghany M 2002 *Appl. Phys. Lett.* **81** 1534
[49] Seyller Th, Sieber N, Stark T, Ley L, Zorman C and Mehregany M 2003 *Surf. Sci.* **532–535** 698
[50] Kimoto T, Itoh A, Matsunami H and Okano T 1997 *J. Appl. Phys.* **81** 3494
[51] Starke U 1997 *Phys. Status Solidi* b **202** 475
[52] Starke U, Bernhardt J, Franke M, Schardt J and Heinz K 1997 *Diamond Relat. Mater.* **6** 1349
[53] Schardt J, Bernhardt J, Franke M, Starke U and Heinz K 1998 *Mater. Sci. Forum* **264–268** 343
[54] Schardt J, Bernhardt J, Starke U and Heinz K 1998 *Surf. Rev. Lett.* **5** 181
[55] Ishida Y, Takahashi T, Okumura H, Yoshida S and Sekigawa T 1997 *Japan. J. Appl. Phys.* **36** 6633
[56] Hara S, Meguro T, Aoyagi Y, Kawai M, Misawa S, Sakuma E and Yoshida S 1993 *Thin Solid Films* **225** 240
[57] Takahashi K, Uchida M, Kitabatake M and Uenoyama T 2000 *Mater. Sci. Forum* **338–342** 141
[58] Starke U, Schardt J, Bernhardt J, Franke M and Heinz K 1999 *Phys. Rev. Lett.* **82** 2107
[59] Virojanadara C and Johansson L 2002 *Surf. Sci.* **519** 73
[60] Sabisch M, Krüger P and Pollmann J 1997 *Phys. Rev.* B **55** 10561
[61] Bernhardt J, Nerding N, Starke U and Heinz K 1999 *Mater. Sci. Eng.* B **61/62** 207
[62] Forbeaux I, Themlin J-M and Debever J-M 1999 *Surf. Sci.* **442** 9
[63] Pollmann J, Krüger P and Sabisch M 1997 *Phys. Status Solidi* b **202** 421
[64] Johansson L I, Owman F and Martensson P 1996 *Surf. Sci.* **360** L478
[65] Hüsken H, Schröter B and Richter W 1998 *Surf. Sci.* **407** L676
[66] Hubbard J 1963 *Proc. R. Soc.* A **276** 238
[67] Hubbard J 1964 *Proc. R. Soc.* A **277** 237

[68] Hubbard J 1964 *Proc. R. Soc.* A **281** 401
[69] Mott N F 1949 *Proc. R. Soc.* A **62** 416
[70] Flores F, Ortega J and Pérez R 1999 *Surf. Rev. Lett.* **6** 411
[71] Rohlfing M and Pollmann J 2000 *Phys. Rev. Lett.* **84** 135
[72] Furthüller J, Bechstedt F, Hüsken H, Schröter B and Richter W 1998 *Phys. Rev.* B **58** 13712
[73] Zangwill A 1988 *Physics at Surfaces* (Cambridge: Cambridge University Press)
[74] Sze S 1981 *Physics of Semiconductor Devices* (New York: Wiley)
[75] Ching W, Lam D and Lin C 1980 *Phys. Rev.* B **21** 2378
[76] Economou E and Papaconstantopoulos D 1981 *Phys. Rev.* B **23** 2042
[77] Widstrand S, Johansson L, Magnusson K, Larson M, Yeom H, Hara S and Yoshida S 2001 *Surf. Sci.* **479** 247
[78] Afanas'ev V V, Bassler M, Pensl G, Schulz M and von Kamienski E S 1996 *J. Appl. Phys.* **79** 3108
[79] Patrick L and Choyke W 1972 *Phys. Rev.* B **2** 2255
[80] Gao K, Seyller Th, Ley L, Ciobanu F, Pensl G, Tadich A, Riley J D and Leckey R G C 2003 at press